

Numerical integration of quasi-linear hyperbolic PDEs governing the inverse dynamics of flexible mechanical systems

Timo Ströhle and Peter Betsch

Institute of Mechanics
Karlsruhe Institute of Technology, Karlsruhe, Germany
timo.stroehle@kit.edu, peter.betsch@kit.edu

ABSTRACT

This work is concerned with the inverse dynamics of flexible mechanical systems whose motion is governed by quasi-linear hyperbolic partial differential equations. It appears, that classical solution strategies, i.e. sequential space-time integration lead to serious issues, that will be addressed. Motivated by the hyperbolic structure of the underlying initial boundary value problem, two novel methods based on a simultaneous space-time integration will be presented. Thereby, special attention will be paid to the phenomena of wave propagation within spatially continuous mechanical systems and its relevance regarding the inverse dynamics problem.

Keywords: Inverse dynamics, Quasi-linear hyperbolic PDEs, Method of characteristics, Wave propagation, Galerkin space-time integration, Geometrically exact beam formulation.

1 FORMULATION OF THE PROBLEM

We focus on the inverse dynamics of underactuated flexible mechanical systems whose motion is governed by hyperbolic partial differential equations of the form

$$A\partial_t^2 x - \operatorname{div}_s(B\partial_s x) = C. \quad (1)$$

We furthermore assume quasi-linearity, i.e. the coefficients A, B and C are explicitly allowed to depend on the space and time variables $s \in S \subset \mathbb{R}^\alpha$ and $t \in T = [0, \infty)$ as well as on the solution $x : S \times T = \Omega \subset \mathbb{R}^{\alpha+1} \mapsto \mathbb{R}^d$ and its first partial derivatives, i.e.

$$A, B : \bar{\Omega} \mapsto \mathbb{R}^{d,d} \quad \text{and} \quad C : \bar{\Omega} \mapsto \mathbb{R}^d \quad \text{where} \quad \bar{\Omega} = \Omega \cup \{(x, \partial_s x, \partial_t x) : \Omega \mapsto \mathbb{R}^d\}. \quad (2)$$

Since we are interested in the inverse dynamics problem, we ask for the unknown *Neumann*-boundary conditions

$$B\partial_s x(\partial\Omega_f) = f(t). \quad (3)$$

on $\partial\Omega_f = \partial S_f \times T$, such that, some given time-variant *Dirichlet*-boundary conditions on $\partial\Omega_\gamma = \partial S_\gamma \times T$

$$x(\partial\Omega_\gamma) = \gamma(t) \quad (4)$$

are fulfilled. In (3) and (4), the unknown actuation $f(t) : \partial\Omega_f \mapsto \mathbb{R}^d$, acting on $\partial\Omega_f$ and the partly prescribed motion $\gamma(t) : \partial\Omega_\gamma \mapsto \mathbb{R}^d$ on $\partial\Omega_\gamma$, has been introduced, respectively. In case of flexible multibody dynamics, additionally *Neumann* boundary conditions might be imposed on $\partial\Omega_\gamma = \partial S_\gamma \times T$

$$B\partial_s x(\partial\Omega_\gamma) = n(t). \quad (5)$$

Herein $n(t) : \partial\Omega_\gamma \mapsto \mathbb{R}^d$ denotes the contact force acting on $\partial\Omega_\gamma$. Initial conditions

$$x(\partial\Omega_0) = x_0(s) \quad \text{and} \quad \partial_t x(\partial\Omega_0) = v_0(s) \quad \forall \quad s \in S \quad (6)$$

are imposed on $\partial\Omega_0 = S \times \{0\}$. See Fig. 1 for an illustration of the underlying space-time domain.

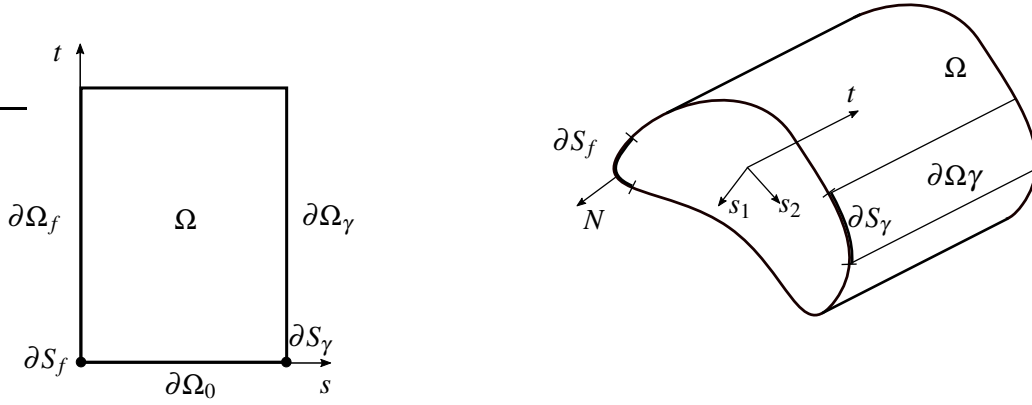


Figure 1. Space-time domain for $\alpha = 1$ (left) and $\alpha = 2$ (right).

Example 1.1 (Geometrically exact beam formulation). *Subsequently, the ‘classical equations of motion of geometrically exact beams’ are briefly derived. Furthermore it will be shown, that these equations indeed fit into the proposed framework introduced in the beginning of this Section. Essentially, these derivations are based on the work published in [1], [2], [3] and [4].*

Kinematics. The motion of every material point $s \in S = [0, 1] \subset \mathbb{R}$ of the beam for every point in time $t \in T = [0, \infty) \subset \mathbb{R}$ is defined by the deformation map¹

$$r : \Omega \equiv S \times T \mapsto \mathbb{R}^3$$

together with the moving orthonormal basis

$$d_i : \Omega \mapsto \mathbb{R}^3 \quad \forall i \in \{1, 2, 3\}.$$

Furthermore, we define in the reference configuration

$$R(s) \equiv r(\partial\Omega_0) : \partial\Omega_0 \mapsto \mathbb{R}^3 \quad \text{and} \quad D_i(s) \equiv d_i(\partial\Omega_0) : \partial\Omega_0 \mapsto \mathbb{R}^3.$$

By introducing the proper-orthogonal tensor $\Lambda \in SO(3)$, the rotation of the orthonormal basis is given by

$$d_i = \Lambda D_i. \quad (7)$$

Note that the orthonormal basis d_i indicates the ‘average orientation of the cross-section’, whereby d_3 is normal and d_1 and d_2 are tangential to the cross-section. It may be worth to emphasize at this point, that planarity of the cross-section is assumed. Abandoning this assumption would require a further spatial variable. A spatial differentiation of the moving frame yields

$$\partial_s d_i = (\partial_s \Lambda) D_i + \Lambda \partial_s D_i = (\partial_s \Lambda) \Lambda^T d_i + \Lambda (\partial_s \Lambda_0) \Lambda_0^T \Lambda^T d_i. \quad (8)$$

Here, use of the product rule and $D_i = \Lambda_0 e_i$ has been made. Introducing the skew-symmetric curvature matrix²

$$S_\kappa(\Theta) = (\partial_s \Lambda(\Theta)) \Lambda^T(\Theta) = \begin{bmatrix} 0 & -\kappa_3 & \kappa_2 \\ \kappa_3 & 0 & -\kappa_1 \\ -\kappa_2 & \kappa_1 & 0 \end{bmatrix} \quad (9)$$

equation (8) can be rewritten as

$$\partial_s d_i = (S_\kappa(\Theta) + \Lambda S_\kappa(\Theta_0) \Lambda^T) d_i = \bar{S}_\kappa(\Theta, \Theta_0) d_i. \quad (10)$$

¹Note, that the deformation map $r(\Omega)$ must not necessarily coincides with the line of centroids of the beam.

²Orthogonality of Λ implies $\Lambda \Lambda^T = I$. Differentiation of this orthogonality condition with respect to s yields $\partial_s(\Lambda) \Lambda^T + \Lambda \partial_s(\Lambda^T) = 0$ indicating the skew-symmetry of $\partial_s(\Lambda) \Lambda^T$

Note that assuming a straight reference configuration implies $S_{\kappa}(\Theta_0) = 0$. Introducing the axial vector $\kappa = \kappa_i d_i$, equation (10) can be defined alternatively as

$$\partial_s d_i = \kappa \times d_i.$$

The same relations hold for the temporal change of the moving basis

$$\partial_t d_i = S_{\omega}(\Theta, \Theta_0) d_i = \omega \times d_i,$$

where S_{ω} represents the skew symmetric angular velocity matrix. Following [1], we define the strain variables $\gamma_i = \partial_s r \cdot d_i$ and κ_i , where γ_1 and γ_2 measure shear, γ_3 measures dilatation, κ_1 and κ_2 measure flexure and κ_3 measures torsion.

Equilibrium. After having adressed the kinematics in the last Section, the corresponding dynamics will be investigated in the following Section. The (material form of the) balance of linear momentum on an interval $S \supset I = [c, s]$ of the beam can be established as follows

$$n(s, t) - n(c, t) + \int_c^s \bar{n}(\xi_3) d\xi_3 = \partial_t P(s, t). \quad (11)$$

Herein the contact force has been defined as $n : \Omega \mapsto \mathbb{R}^d$, the external load as $\bar{n} : \Omega \mapsto \mathbb{R}^d$ and the linear momentum of the considered beam segment as $P : \Omega \mapsto \mathbb{R}^d$ which can be stated for the center of gravity $r_S = r + \xi_{\alpha}^S d_{\alpha}$ as

$$\begin{aligned} P(s, t) &= \int \partial_t r_S dm \\ &= \int_c^s (\rho A)(s) \partial_t r + (\rho S_{\alpha})(s) \partial_t d_{\alpha} d\xi_3 \quad \forall \alpha \in \{1, 2\} \\ &= \int_c^s p(s, t) d\xi_3. \end{aligned} \quad (12)$$

Here, we used the fact that the center of gravity of each cross-section is defined by the components $\xi_{\alpha}^S = A^{-1} \int \xi_{\alpha} dA = A^{-1} S_{\alpha}$, where $S_{\alpha} \forall \alpha \in \{1, 2\}$ is the first moment of area with respect to ξ_{α} . Time derivative of the linear momentum yields

$$\partial_t p(s, t) = (\rho A)(s) \partial_t^2 r + \partial_t^2 q, \quad (13)$$

where use of the definition of the linear momentum relative to $r(s, t)$

$$\partial_t q(s, t) \equiv (\rho S_{\alpha})(s) \partial_t d_{\alpha} \quad \forall \alpha \in \{1, 2\}$$

has been made. Obviously, the relative linear momentum vanishes by choosing $r(s, t)$ accurate. Furthermore, for the same beam segment, the material form of the balance of angular momentum can be established in the form

$$\begin{aligned} m(s, t) - m(c, t) + (r(s, t) \times n(s, t)) - (r(c, t) \times n(c, t)) \\ + \int_c^s r(\xi) \times \bar{n}(\xi) d\xi + \int_c^s \bar{m}(\xi) d\xi = \partial_t L(s, t). \end{aligned} \quad (14)$$

Herein, we introduced the contact torque $m : \Omega \mapsto \mathbb{R}^3$, the external applied torques $\bar{m} : \Omega \mapsto \mathbb{R}^3$ and the angular momentum (with respect to a fixed point in space) of the considered beam segment $L : \Omega \mapsto \mathbb{R}^3$ which can be stated with $r_P = r + \xi_{\alpha} d_{\alpha}$ as

$$\begin{aligned} L(s, t) &= \int r_P \times \partial_t(r_P) dm \\ &= \int_c^s \rho A (r \times \partial_t r) + \rho S_{\alpha} (r \times \partial_t d_{\alpha} + d_{\alpha} \times \partial_t r) + \rho I_{\alpha} (d_{\alpha} \times \partial_t d_{\alpha}) d\xi_3 \\ &= \int_c^s l(s, t) d\xi_3. \end{aligned} \quad (15)$$

Herein, $l(s,t)$ denotes the angular momentum density. Its time derivative is

$$\partial_t l(s,t) = \rho A(r \times \partial_t^2 r) + r \times \partial_t^2 q + q \times \partial_t^2 r + \partial_t h, \quad (16)$$

where use has been made of the definition of the angular momentum relative to $r(s,t)$,

$$h(t) \equiv \rho I_{\alpha\beta} (d_\alpha \times \partial_t d_\beta)$$

and the standard properties of the vector product $a \times b = -b \times a$ and $a \times a = 0$. Furthermore, we have introduced the second moment of area $I_{\alpha\beta} = \int \xi_\alpha \xi_\beta \, dA$. Differentiating (11) and (14) with respect to the spatial variable $s \in S$, the balance equations can be written as

$$\begin{aligned} \partial_s n + \bar{n} &= \partial_t p \\ \partial_s m + (r \times \partial_s n) + (\partial_s r \times n) + (r \times \bar{n}) + \bar{m} &= \partial_t l. \end{aligned} \quad (17)$$

Using equation (17)₁ together with (13) the following relation can be established

$$r \times \partial_t p = \rho A(r \times \partial_t^2 r) + r \times \partial_t^2 q = r \times \partial_s n + r \times \bar{n}$$

to reformulate equation (17)₂ as

$$\partial_s m + \partial_s r \times n + \bar{m} = \partial_t \hat{l}, \quad (18)$$

where $\partial_t \hat{l} = q \times \partial_t^2 r + \partial_t h$ has been introduced. Equation (17)₁ and (18) are the 'equations of motion for (the classical form of Cosserat) rods' (cf. [1]). In the following it will be shown, that the classical equations of motion for Cosserat rods aligns with the framework postulated above. For this, the contact forces and moments can be written alternatively as

$$n = N_i d_i = N_i \bar{\Lambda} e_i \quad \text{and} \quad m = M_i \bar{\Lambda} e_i.$$

Focusing on hyperelastic materials, the constitutive relations are governed by the stored energy function $\Psi = \hat{\Psi}(\gamma, \kappa)$. We assume that

$$\begin{aligned} N_i &= \partial_{\gamma_i} \Psi(\gamma, \kappa) = \hat{N}_i(\gamma, \kappa) = F_{ik}(\gamma, \kappa) \gamma_k \\ M_i &= \partial_{\kappa_i} \Psi(\gamma, \kappa) = \hat{M}_i(\gamma, \kappa) = G_{ik}(\gamma, \kappa) \kappa_k \end{aligned}$$

holds. Note that the fundamental conditions, regarding the limiting deformation cases, have to be fulfilled. Consequently for $\gamma_\alpha \rightarrow \{\pm\infty\}$ the contact force N_α should tend to $\pm\infty$ and the contact force N_3 should tend to $\pm\infty$ for $\gamma_3 \rightarrow \{\infty, 0\}$. The contact moments M_i should tend to $\pm\infty$ as the curvature κ_i tends to an upper or lower bound, where an intersection of neighboring cross-sections is imminent. Taking the kinematical relations

$$\gamma_k = \partial_s r \cdot \bar{\Lambda} e_k \quad \text{and} \quad \kappa_k = \partial_s \Theta \cdot \bar{\Lambda} e_k$$

into account, the contact force can be written as

$$n = F_{ik}(\gamma) \gamma_k (\bar{\Lambda} e_i) = (\bar{\Lambda} F^T \bar{\Lambda}^T) \cdot \partial_s r.$$

Herein, $F = F_{ik}(\gamma)(e_i \otimes e_k)$ has been introduced and use of $Ae_j \otimes Ae_i = A(e_i \otimes e_j)A^T$ has been made³. For the contact moment, it follows similarly that $m = (\bar{\Lambda} G^T \bar{\Lambda}^T) \cdot \partial_s \Theta$. With

$$\partial_t^2 d_\alpha = S_\omega^2 d_\alpha - d_\alpha \times \partial_t \omega$$

the time derivative of the linear momentum relative to $r(s,t)$ can be written as

$$\partial_t^2 q(s,t) = S_\omega^2 q - S_q \partial_t^2 \Theta,$$

³This property follows directly from the definition of the dyadic product $(a \cdot b)c = (c \otimes a)b$

where $S_{(\cdot)}$ denotes the skew symmetric matrix

$$S_{(\cdot)} = \begin{bmatrix} \mathbf{0} & -(\cdot)_3 & (\cdot)_2 \\ (\cdot)_3 & \mathbf{0} & -(\cdot)_1 \\ -(\cdot)_2 & (\cdot)_1 & \mathbf{0} \end{bmatrix},$$

such that $S_\omega \omega \equiv 0$ holds by definition. Hence, the balance of linear momentum (17)₁ can be written as

$$(\rho A) \partial_t^2 r - S_q \partial_t^2 \Theta - \partial_s (\Lambda F^T \Lambda^T \partial_s r) = \bar{n} - S_\omega^2 q.$$

Furthermore, by using the relation for the angular momentum relative to $r(s, t)$ and its time derivative

$$\partial_t h(s, t) = \rho I_{\alpha\beta} \partial_t (d_\alpha \times \partial_t d_\beta),$$

equation (17)₂ can be written by defining $J \equiv I_{\alpha\beta} S_{d_\alpha} S_{d_\beta}$ and $k \equiv I_{\alpha\beta} (d_\alpha \times S_\omega^2 d_\beta + \omega \cdot (d_\alpha \times d_\beta) \omega)$ as

$$S_q \partial_t^2 r - \rho J \partial_t^2 \Theta + \Lambda G^T \Lambda^T = \partial_s r \times n + \bar{m} - \rho k.$$

By introducing the coefficients

$$A = \begin{bmatrix} \rho A I & -S_q \\ S_q & -\rho J \end{bmatrix}, \quad B = \begin{bmatrix} \bar{\Lambda} F^T \bar{\Lambda}^T & \mathbf{0} \\ \mathbf{0} & \bar{\Lambda} G^T \bar{\Lambda}^T \end{bmatrix} \quad \text{and} \quad C = \begin{bmatrix} \bar{n} - S_\omega^2 q \\ (\partial_s r \times n) + \bar{m} - \rho k \end{bmatrix},$$

the problem aligns with the framework presented above.

2 SEQUENTIAL SPACE-TIME INTEGRATION

Commonly, initial boundary value problems in form of (1) are solved sequentially in space and time: The underlying partial differential equation (1) is first integrated in space by applying common methods such as the finite element method, before the semi-discrete system of equations can be solved in time by using appropriate time-stepping schemes that are commonly based on finite difference approximations. Following this classical procedure we demonstrate that the inverse dynamics problem under consideration can be transferred to (spatially) discrete equations of motion subjected to servo-constraints. For this we consider the pure *Neumann* problem, i.e. *Dirichlet*-boundary conditions are neglected. An equivalent weak form of the boundary value problem at hand can be accomplished by multiplying (1)₁ by sufficiently smooth test functions, integrating subsequently over the spatial domain S , applying integration by parts and taking finally the given *Neumann* boundary conditions into account. A spatial discretization of the weak form, by applying standard finite element approximations to the vector valued test and trial functions, leads to semi-discrete equations of motion. Boundary conditions pertaining the configuration space may then be taken into account by imposing geometric constraints. In the case of the inverse dynamics problem, the unknown *Neumann*-boundary conditions (3) can be considered as Lagrange multipliers enforcing the prescribed, time-varying *Dirichlet*-boundary condition. The motion of such systems (without assuming any further geometric constraints) are governed by the following differential algebraic equation (DAE)

$$\begin{aligned} M D_t^2 q(t) + F(D_t q(t), q, t) + G^T f(t) &= 0 \\ g(q, t) = H q(t) - \gamma(t) &= 0. \end{aligned} \tag{19}$$

Herein the nodal configuration vector $q : T \mapsto \mathbb{R}^k$ and the actuating components $f : T \mapsto \mathbb{R}^m$, for $m < k$ have been introduced. We will show that due to the spatially disjunct, hence non-standard construction of the constraint realization, the resulting DAEs are in general characterized by either a high differentiation index or the appearance of (unstable) internal dynamics, depending on the spatial discretization. For mechanical systems that are subjected to classical contact constraints, i.e. $H = G$, the constraint forces are observed to be ideal orthogonal to the constraint manifold

$Q = \{q : g(q, t) = 0\}$. Such systems can be identified as Hessenberg systems with differentiation index $\nu_d = 3$ (cf. [5], Chapter 4, p.172). The semi discrete equation of motion can then be solved by integrating (19) subsequently in time by applying suitable finite difference schemes.

In contrast to that, servo-constraints (19)₂ in general do not have collocation property. Geometrically this means, that the constraint forces are not orthogonal to the constraint manifold Q anymore. The geometrical properties of different constraint realizations are specified by

$$n = \text{rank}(HM^{-1}G^T). \quad (20)$$

Three distinct cases of the resulting orientation of the actuation $G^T f(t)$ on the constraint manifold Q can be identified (cf. e.g. [6]):

- (i) $n = m$ (Non-ideal) orthogonal.
All m constraint components can be actuated
- (ii) $0 < n < m$ Mixed orthogonal-tangential.
Only n constraint components can be actuated directly.
- (iii) $n = 0$ Tangential.
None of the constraint components can be actuated directly.

Orthogonal constraint realizations lead to differentially non-flat systems, where (unstable) internal dynamics may arise. For mixed orthogonal-tangential and fully tangential constraint realizations, the system at hand is possibly differentially flat or non-flat, either without or with internal dynamics. In case of non-flat systems (unstable) inverse dynamics may occur, hindering numerical integration of the problem at hand. Therefore, it is inevitable to carry out relevant analysis thereof (cf. [7] and [8]). On the other hand, flat systems lead to DAEs, that are characterized by high differentiation index. In addition to that, the demands on the smoothness of the prescribed trajectory tend to be excessively high as well. Since a numerically stable solution of the resulting DAEs is depending significantly on the differentiation index, it is inevitable to reduce the index in order to get a stable numerical solution (cf. [9] and references therein). This obviously restricts the applicability of the classical semi-discretization approaches.

Therefore, we aim to analyse the initial boundary value problem in more detail - exposing the underlying hyperbolic structure of the governing partial differential equations anticipates to gain more insights into the problem at hand. By enlightening resulting mechanisms such as wave propagation, it will become more and more apparent, that a simultaneous space-time integration is much better suited to successfully solve the inverse dynamics problem under consideration numerically stable (cf. [10]). In fact, it will be demonstrated, that both, internal dynamics and high differentiation index DAEs are caused by the sequential discretization process, leading to incomplete boundary data and consequently to an ill-posed problem. Motivated by this new insights, we will be able to present two novel numerical methods based on a simultaneous space-time integration of the initial boundary value problem at hand.

3 SIMULTANEOUS SPACE-TIME INTEGRATION

Due to the highly restrictive applicability of solving the control problem at hand sequentially in time, two methods will be presented in this Section, that are based on a simultaneous space-time integration. This will be motivated by the hyperbolic structure of the underlying initial boundary value problem. For this, the classical method of characteristics will be introduced in the subsequent Section.

Method of characteristics. The method of characteristics is based on a geometric interpretation of quasi-linear partial differential equations (cf. [11] and [12]). For this the wave equation for the

control problem at hand (1) is transformed into a system of first order partial differential equations by introducing the velocity $v(s,t) = \partial_t x(s,t)$ and the deformation gradient $p(s,t) = \partial_s x(s,t)$

$$A \partial_t v - \partial_s (Bp) = C \quad (21)$$

$$B \partial_t p - B \partial_s v = 0. \quad (22)$$

With $B \partial_t p = \partial_t (Bp) - \partial_t B p$ equation (22) can be written as $\partial_t (Bp) - B \partial_s v = \partial_t B p$. Together with

$$\partial_t B(p(s,t)) = (\partial_p \otimes B) \cdot \partial_t p = \text{grad}_p(B) \cdot \partial_t p$$

and by using the equality of mixed partials $\partial_t p = \partial_s v$ it follows that

$$\partial_t (Bp) - B \partial_s v = (\partial_p \otimes B) p \partial_s v \quad (23)$$

holds. Equation (21) is forming together with (23) and

$$B + (\partial_p \otimes B) p = H(p) : \bar{\Omega} \mapsto \mathbb{R}^{d,d} \quad (24)$$

a system of first order partial differential equations. Introducing $z : \Omega \mapsto \mathbb{R}^{2d}$, $F : \bar{\Omega} \mapsto \mathbb{R}^{2d}$, $D : \bar{\Omega} \mapsto \mathbb{R}^{2d,2d}$ and $E : \bar{\Omega} \mapsto \mathbb{R}^{2d,2d}$, this system can be written compactly as:

$$D \partial_t z + E \partial_s z = F. \quad (25)$$

Assuming there exists a line $s = k(t)$ along which a solution $z = z(k(t), t) = z_0(t)$ is given. Then this line is called a characteristic line if the partial derivatives of the solution cannot be uniquely determined through informations along this given line. This means that

$$\left(E - D \frac{d}{dt} k(t) \right) \partial_s z = F - D \frac{d}{dt} z_0(t) \quad (26)$$

cannot be solved uniquely for the partial derivatives $\partial_s z$ and $\partial_t z$. Hence, according to Cramers rule

$$\det(Q) = 0 \quad \text{and} \quad \det(Q)_i = 0 \quad (27)$$

has to hold for the coefficient matrix $Q = E - D \frac{d}{dt} k(t)$ as well as for the matrix Q_i , where the i -th column is replaced by the right hand side $F - D \frac{d}{dt} z_0(t)$. The wave equation could thus be transformed into a system of ordinary differential equations along characteristic lines. This system can be solved numerically by using e.g. appropriate finite difference schemes.

Example 3.1 (Planar problem). *The wave propagation within the planar formulation of the geometrically exact beam can be analysed by evaluating*

$$(\partial_p \otimes B) p = \frac{EA}{v^2} \begin{bmatrix} \cos^2 \Theta & \cos \Theta \sin \Theta & 0 \\ \cos \Theta \sin \Theta & \sin^2 \Theta & 0 \\ 0 & 0 & 0 \end{bmatrix} \quad (28)$$

and

$$H = \frac{EA}{2} (1 + v^{-2}) \begin{bmatrix} \cos^2 \Theta & \cos \Theta \sin \Theta & 0 \\ \cos \Theta \sin \Theta & \sin^2 \Theta & 0 \\ 0 & 0 & 0 \end{bmatrix} + \begin{bmatrix} GA \sin^2 \Theta & -GA \cos \Theta \sin 2\Theta & 0 \\ -GA \cos \Theta \sin 2\Theta & GA \cos^2 \Theta & 0 \\ 0 & 0 & EI \end{bmatrix}$$

for the given coefficients. The directionality condition (27) leads then to

$$c_1 = \pm \left(\frac{EI}{\rho I} \right)^{\frac{1}{2}}, \quad c_2 = \pm \left(\frac{GA}{\rho A} \right)^{\frac{1}{2}} \quad \text{and} \quad c_3 = \pm \left(\frac{1}{2} \frac{EA}{\rho A} \left(1 + \frac{1}{\gamma_3^2} \right) \right)^{\frac{1}{2}}. \quad (29)$$

Here, c_i can be identified as the speed of wave propagation corresponding to bending ($i = 1$), shear ($i = 2$) and elongation ($i = 3$), respectively. It is worth to mention, that the compatibility condition (27)₂ yields a system of ordinary differential equations along the characteristic lines (27)₁. Following [10] and references therein, this system of ODEs can be solved globally in the space-time domain Ω .

Space-time finite element method. Due to the gained insights of the underlying wave dominated problems, a space-time finite element method will be presented in this paragraph. For further information we would like to refer to [10] as well as [13] and [14]. By introducing the velocity $v(s, t) = \partial_t x(s, t)$, the underlying partial differential equation at hand (1) can be transformed into a system of partial differential equations, that is first order in time:

$$\begin{aligned} \partial_t x - v &= 0 \\ A \partial_t v - \partial_s (B \partial_s x) &= C. \end{aligned} \quad (30)$$

Multiplying each equation in (30) with sufficiently smooth test functions $w_1(s, t)$ and $w_2(s, t)$, integrating over the space-time domain $\Omega = S \times T$ and applying integration by parts to the second integral of (30)₂ regarding the spatial variable

$$\int_{\Omega} w_2 \cdot \partial_s (B \partial_s x) d\Omega = \int_T [w_2 \cdot B \partial_s x]_{s=0}^1 dt - \int_{\Omega} \partial_s w_2 \cdot B \partial_s x d\Omega \quad (31)$$

yields the following weak formulation:

$$\begin{aligned} \int_{\Omega} w_1 \cdot (\partial_t x - v) d\Omega &= 0 \\ \int_{\Omega} w_2 \cdot A \partial_t v d\Omega - \int_T [w_2 \cdot B \partial_s x]_{s=0}^1 dt + \int_{\Omega} \partial_s w_2 \cdot B \partial_s x d\Omega &= \int_{\Omega} w_2 \cdot C d\Omega. \end{aligned} \quad (32)$$

Additionally the servo-constraint $g_c(t) = x(1, t) - \gamma(t) = 0$ can be demanded weakly on the boundary $\partial\Omega_{\gamma} = \{1\} \times T$

$$\int_{\partial\Omega_{\gamma}} w_3(t) \cdot g_c(t) dt = 0. \quad (33)$$

The task is now to find the unknown functions

$$\begin{aligned} x(s, t) &\in V_1 = \left\{ x : \Omega \mapsto \mathbb{R}^d \mid x(\partial\Omega_0) = x_0 \right\} \\ v(s, t) &\in V_2 = \left\{ v : \Omega \mapsto \mathbb{R}^d \mid v(\partial\Omega_0) = v_0 \right\} \\ f(t) &\in V_3 = \left\{ f : \partial\Omega_f \mapsto \mathbb{R}^d \mid f(\partial\Omega_f \cap \partial\Omega_0) = f_0 \right\} \end{aligned}$$

such that for arbitrary but sufficiently smooth test functions

$$\begin{aligned} w_1(s, t), w_2(s, t) &\in W_1 = \left\{ w_1, w_2 : \Omega \mapsto \mathbb{R}^d \mid w_1(\partial\Omega_0) = 0, w_2(\partial\Omega_0) = 0 \right\} \\ w_3(t) &\in W_2 = \left\{ w_3 : \partial\Omega_{\gamma} \mapsto \mathbb{R}^d \mid w_3(\partial\Omega_{\gamma} \cap \partial\Omega_0) = 0 \right\} \end{aligned}$$

the equations (32) and (33) are satisfied together with the given boundary and initial conditions. The weak formulation consisting of (32) and (33) subjected to the given *Neumann* and *Dirichlet* boundary conditions can then be solved numerically using the finite element method based on a piecewise continuous approximation.

Example 3.2 (Numerical example). *Regarding a beam with mass density $\rho = 1$ and axial-, bending- and shear stiffness $EA = 1$, $EI = 1$ and $GA = 1$ respectively, the actuation $f = [f_x \ f_y \ m]^T$ acting at $s = 0$ is searched, such that the beam at $s = L$ follows a prescribed trajectory. Furthermore, the length of the beam is assumed to be $L = 1$ in a stress-free reference configuration. A rest-to-rest maneuver starting at $t_0 = 2$ and ending at $t_f = t_0 + T = 4$ is chosen. The prescribed maneuver can therefore be defined by*

$$\gamma = \begin{bmatrix} 1 \\ 0 \\ 0 \end{bmatrix} \forall t < t_0 \quad \gamma = \begin{bmatrix} 1 - \cos(\varphi \cdot s(t)) \\ \sin(\varphi \cdot s(t)) \\ \varphi \cdot s(t) \end{bmatrix} \forall t \in [t_0, t_0 + T] \quad \gamma = \begin{bmatrix} 0 \\ 1 \\ \varphi \end{bmatrix} \forall t > t_f. \quad (34)$$

Here, φ denotes the angle of rotation. Furthermore, the function

$$s(t) = 1 - \frac{1}{2} \left(\cos \left(\frac{\pi}{2} \left(\sin \left(\pi \frac{t-t_0}{T} - \frac{\pi}{2} \right) + 1 \right) \right) + 1 \right)$$

has been introduced.

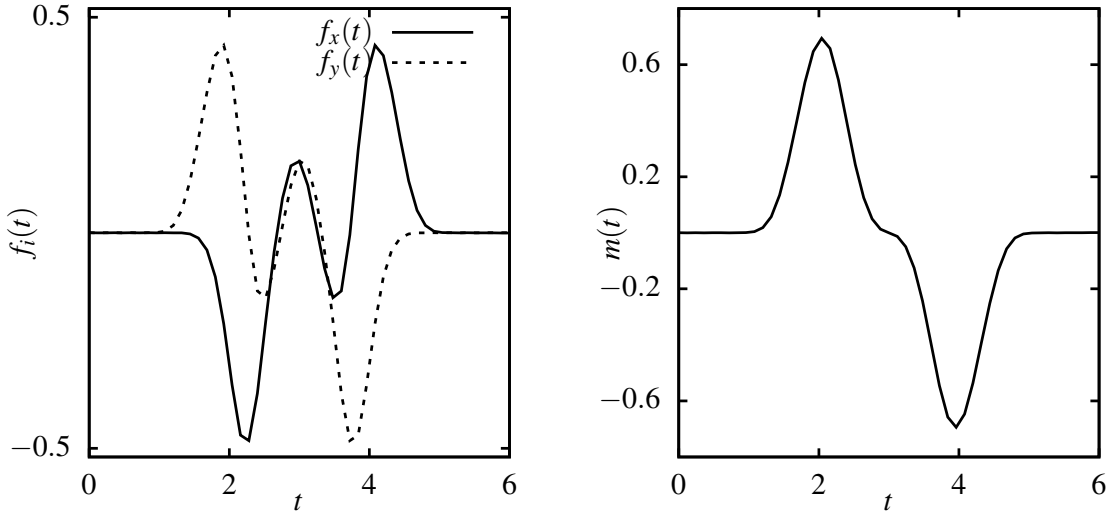


Figure 2. Components of the force (left) and torque (right) acting at $s = 0$ computed with the proposed space-time finite element method such that the beam at $s = L$ follows a prescribed circle from $P_0(1,0)$ to $P_T(0,1)$

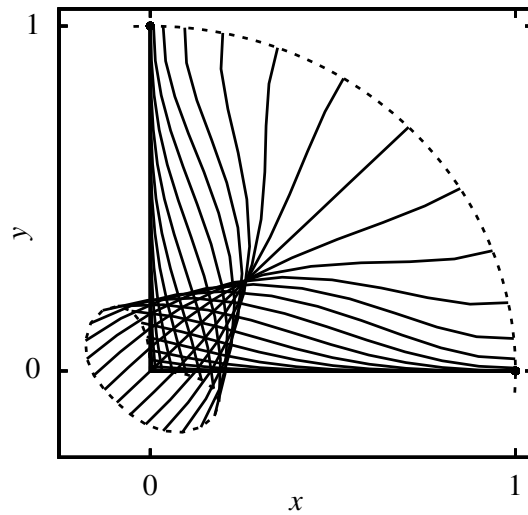


Figure 3. Snapshots of the circular rest-to-rest motion.

In Figure 2 the components of the actuating force f_i (left) and the actuating torque m (right) is depicted. Note, that also the delay time can be observed herein. This is due to the hyperbolic structure of the underlying system mentioned earlier. In Figure 3 snapshots of the planar motion of the beam satisfying the prescribed trajectory at $s = L$ are shown.

4 CONCLUSION

In this work, the inverse dynamics of flexible mechanical systems whose motion is governed by quasi-linear partial differential equations of hyperbolic type has been investigated. Therefore, the governing initial boundary value problem has been introduced first abstractly in Section 1, before the equations of motion for the classical form of *Cosserat* rods, have been derived briefly, aligning with the postulated framework. In Section 2, problems that occur by solving the initial boundary value problem at hand by using classical sequential space-time integration methods has been addressed. In particular, the role of the given servo-constraints causing these problems has been pointed out by identifying crucial differences to ordinary contact-constraints. In Section 3 simultaneous space-time integration methods could be presented that are highly motivated by the wave phenomena within elastic media. For this characteristic lines could be identified, giving the direction of the propagation of informations within the corresponding space-time domain. Inspired by these insights, two methods that are capable to solve the inverse dynamics of flexible mechanical systems numerically stable has been introduced.

REFERENCES

- [1] Antman, S.: *Nonlinear Problems of Elasticity*. 2nd edn. Springer (2005)
- [2] Simo, J.: A finite strain beam formulation. The three-dimensional dynamic problem. Part I. *Computer Methods in Applied Mechanics and Engineering* **49**(1) (1985) 55–70
- [3] Reissner, E.: On one-dimensional finite-strain beam theory: The plane problem. *Journal of Applied Mathematics and Physics (ZAMP)* **23** (1972) 795—804
- [4] Betsch, P., Steinmann, P.: Frame-indifferent beam finite elements based upon the geometrically exact beam theory. *International Journal for Numerical Methods in Engineering* **54**(12) (2002) 1775–1788
- [5] Kunkel, P., Mehrmann, V.: *Differential-Algebraic Equations - Analysis and Numerical Solution*. EMS Textbooks in Mathematics (2006)
- [6] Blajer, W., Kołodziejczyk, K.: A geometric approach to solving problems of control constraints: Theory and a DAE framework. *Multibody System Dynamics* **11** (2004) 343–364
- [7] Berger, T., Drücker, S., Lanza, L., Reis, T., Seifried, R.: Tracking control for underactuated non-minimum phase multibody systems. *Nonlinear Dynamics* **104** (2021) 3671–3699
- [8] Seifried, R.: Integrated mechanical and control design of underactuated multibody systems. *Nonlinear Dynamics* **67** (2012) 1539–1557
- [9] Altmann, R., Betsch, P., Yang, Y.: Index reduction by minimal extension for the inverse dynamics simulation of cranes. *Multibody System Dynamics* **36**(3) (2016) 295–321
- [10] Ströhle, T., Betsch, P.: A simultaneous space-time discretization approach to the inverse dynamics of geometrically exact strings. *International Journal for Numerical Methods in Engineering* **123**(11) (2022) 2573–2609
- [11] Courant, R., Friedrichs, K.O.: *Supersonic Flow and Shock Waves*. Interscience (1948)
- [12] John, F.: *Partial Differential Equations*. Springer (1982)
- [13] Argyris, J.H., Scharpf, D.W.: Finite elements in time and space. *Nuclear Engineering and Design* **10** (1969) 456–464
- [14] Hughes, T.J.R., Hulbert, G.M.: Space-time finite element methods for elastodynamics: Formulations and error estimates. *Computer Methods in Applied Mechanics and Engineering* **66** (1988) 339–363